Distribution Agreement

In presenting this thesis as a partial fulfillment of the requirements for a degree from Emory University, I hereby grant to Emory University and its agents the non-exclusive license to archive, make accessible, and display my thesis in whole or in part in all forms of media, now or hereafter now, including display on the World Wide Web. I understand that I may select some access restrictions as part of the online submission of this thesis. I retain all ownership rights to the copyright of the thesis. I also retain the right to use in future works (such as articles or books) all or part of this thesis.

Amy Seung Hyun Kim March 24, 2023

The Role of Fibro/Adipogenic Progenitors for Tongue Muscle Remodeling by High-Fat Diet

By

Amy Seung Hyun Kim

Hyojung Choo
Adviser

Biology

Hyojung Choo
Adviser

Michal Arbilly
Committee Member

Andreas Fritz
Committee Member

Hyojung Choo
Committee Member

2023

The Role of Fibro/Adipogenic Progenitors for Tongue Muscle Remodeling by High-Fat Diet

By

Amy Seung Hyun Kim

Hyojung Choo
Adviser

An abstract of
a thesis submitted to the Faculty of Emory College of Arts and Sciences
of Emory University in partial fulfillment
of the requirements of the degree of
Bachelor of Science with Honors

Biology

2023

Abstract

The Role of Fibro/Adipogenic Progenitors for Tongue Muscle Remodeling by High-Fat Diet
By Amy Seung Hyun Kim

Obstructive sleep apnea (OSA) is a common sleep disorder characterized by repeated episodes of upper airway collapse during sleep, resulting in fragmented sleep and oxygen deprivation. Although obesity is a major cause of OSA by increasing tongue fat, the cellular and molecular mechanisms underlying fat deposition in the tongue of OSA patients have not been well explored. We aim to establish a preclinical model of high-fat tongue in mice fed with a high-fat diet (HFD) for six months as a tool to study the impact of HFD-induced obesity on adipocytes and neuromuscular junctions (NMJs) in tongue muscles. The results demonstrated HFD-induced hypertrophy of adipocytes and denervation at NMJs in tongue muscles. Moreover, we revealed that a mesenchymal stem cell, named fibro/adipogenic progenitors, -derived bone morphogenetic protein-3b (BMP-3b) can drive these changes. BMP-3b maintains NMJ by stabilizing Schwann cells and inhibits the hypertrophy of adipocytes. Our data showed a lower level of *Bmp3b* expression in fibro/adipogenic progenitors of the tongue from HFD-fed mice compared to ND-fed mice. These findings provide important insight into the role of stem cells in the interplay between muscle remodeling, fat deposition, and denervation in the tongue in response to obesity and suggest potential therapeutic targets for OSA treatment. In addition, the study provides a valuable preclinical model for future research to understand the role of fibro/adipogenic progenitors in OSA and related conditions.

The Role of Fibro/Adipogenic Progenitors for Tongue Muscle Remodeling by High-Fat Diet

By

Amy Seung Hyun Kim

Hyojung Choo
Adviser

A thesis submitted to the Faculty of Emory College of Arts and Sciences
of Emory University in partial fulfillment
of the requirements of the degree of
Bachelor of Science with Honors

Biology

2023

Table of Contents

The Role of Fibro/Adipogenic Progenitors for Tongue Muscle Remodeling by High-Fat Diet

Kim, Amy Seung Hyun[1]; Wu, Fang[2]; Choo, Hyojung[2]

[1]Department of Biology, Emory University College of Arts & Sciences,

[2]Department of Cell Biology, Emory University School of Medicine, Atlanta, GA 30322

INTRODUCTION

Obstructive sleep apnea (OSA) is a common sleep-related breathing disorder that affects nearly 1 billion adults globally (Javaheri et al., 2017). It is linked to severe cardiovascular consequences, such as hypertension, heart failure, and stroke (Benjafield et al., 2019) (A. M. Kim et al., 2014). Obesity is a significant risk factor for OSA. Previous clinical study shows that weight loss over a year resulted in significant and clinically relevant improvements in OSA (Foster et al., 2009). Excessive fat deposition at the tongue base is thought to be a possible link between OSA and obesity. A clinical MRI study of OSA patients demonstrated that excessive fat deposition at the tongue base, which is adjacent to the upper airway, causes physical enlargement of the tongue and corresponding upper airway narrowing (A. M. Kim et al., 2014). Although previous clinical studies have established a strong clinical correlation between obesity and OSA through tongue fat deposits (A. M. Kim et al., 2014; Wang et al., 2020), the cellular and molecular mechanism underlying this connection remains unknown mainly due to the lack of preclinical OSA models. Most animal models used in OSA research have focused on observing the consequences of the condition, such as monitoring phenotypes after intermittent hypoxia, rather than exploring the cause of OSA (Trzepizur, Cortese, & Gozal, 2018). While these studies have underscored the importance of OSA treatment, the lack of understanding of the disease's cellular and molecular mechanisms limits the development of potential therapeutics for OSA. Therefore, a preclinical model for investigating the mechanism of OSA is a critical gap in OSA research.

Fibro/adipogenic progenitors (FAPs) have been acknowledged as crucial for maintaining muscles in the limbs and craniofacial regions (E. Kim et al., 2022; Marshall et al., 2019). FAPs play a significant role in supporting neuromuscular junctions (NMJs) and muscle mass, which can be affected by muscle atrophy and NMJ degeneration if there is a depletion of FAPs (E. Kim et al.,

2022; Uezumi et al., 2021). One key molecular mechanism responsible for FAP-regulated muscle maintenance is FAP-derived bone morphogenetic protein-3b (BMP-3b), a member of the transforming growth factor-β superfamily. BMP-3b has been identified as having a function in forming the head in embryos and may be involved in various aspects of skeletal development (Hino, Kangawa, Matsuo, Nohno, & Nishimatsu, 2004). BMP-3b is highly expressed in FAPs and maintains Schwann cell stability (Uezumi et al., 2021). Additionally, BMP-3b has a negative effect on adipocyte hypertrophy. Studies have shown that overexpression of BMP-3b in adipose tissues protects against high-fat diet-induced obesity, while its deficiency is linked with adipocyte hypertrophy (Martí-Pàmies et al., 2020). Furthermore, BMP-3b overexpression has been found to reduce fat infiltration in limb muscles (Kurosawa et al., 2021; Uezumi et al., 2021). However, the role of BMP-3b in fat deposits in tongue muscles remains unknown.

This study aimed to investigate the impact of a high-fat diet (HFD) on fat deposits in tongue muscles and its effect on tongue motion and the integrity of NMJ. We found that HFD feeding caused an increase in adipocyte size and loss of NMJ compared to normal diet (ND) feeding. The reason for this cellular change was found to be a reduction in *Bmp3b* expression in FAPs located in the tongue muscles. This reduction of the gene expression was more noticeable in mice that were fed an HFD compared to those on an ND. The findings suggest that FAP-derived BMP-3b regulates HFD-induced changes in tongue muscles, such as increased fat deposits and denervation. The animal model established by this study provides a platform to explore OSA's cellular and molecular mechanisms and offers opportunities to develop therapeutic interventions for this condition.

METHODS

Animals

C57BL/6J mice (Jax000664) were purchased from Jackson Laboratories (Bar Harbor, ME; www.jax.org). 8-month-old mice were used. Animals were maintained in pathogen-free housing with a 12-h light-dark cycle and ad libitum food and water. Mice received a normal chow diet (ND; Laboratory Rodent Diet 5001), which contains 13.5% of calories from fat until eight weeks of age. Control mice continued on ND while experimental mice switched to a high-fat diet (HFD; Envigo, TD.88137 Adjusted calories diet) containing 42% calories from fat. Mice consumed ND or HFD for six months before analyses. Diabetic B6.BKS(D)-Leprdb/J mice (JAX:000697) were purchased from Jackson Laboratories (Bar Harbor, ME; www.jax.org). Experiments were carried out in accordance with authorized rules and ethical approval from Emory University's Institutional Animal Care and Use Committee, as well as in accordance with the National Institutes of Health.

Lick Assay

Mice were given 48 hours to acclimate to a bottle with a sipper for water consumption. To encourage water drinking during the limited test period, the mice were deprived of water for 16 hours before the experiment. Water bottles were then reintroduced, and lick events were recorded via video approximately 30 seconds later. The iMovie app (Apple) was used to slow down video playback to 0.1X, and tongue protrusions per second for each mouse were measured.

Muscle Tissue Preparation

All muscle tissues were frozen in Tissue-Tek® O.C.T. Compound (Sakura Finetek, Torrance, CA, USA) on N_2-chilled methyl butane and stored at -80C. Cross or longitudinal sections

were prepared to capture adipocytes. Tissue cross sections of 10 μm thickness were collected every 100 - 200 μm using CryoStar NX50 Cryostat (Fisher Scientific, Waltham, MA).

FAPs Isolation and Fluorescence Activated Cell Sorting

To obtain purified FAPs, primary cells were isolated as described previously with small modifications (Cheung et al., 2012). Dissected tongue and gastrocnemius muscles were minced and digested using 0.2% collagenase II (Gibco, Carlsbad, CA) in Dulbecco's modified Eagle's medium (DMEM) at 37°C while shaking at 65 rpm for 90 minutes. Digested fiber suspension was washed and further digested with 0.2% collagenase II (Gibco, Carlsbad, CA) and 2.5 U/ml Dispase II (Gibco, Carlsbad, CA) at 37°C while shaking at 65 rpm for 30 minutes. Digested muscles were then rinsed with the same volume of Hanks' Balanced Salt Solution (HBSS) containing 20% FBS and 100 μg/ml penicillin/streptomycin (P/S). Mononucleated cells were collected using a syringe and 40 μm cell strainer (Thermo Fisher Scientific, Waltham, MA). To label FAPs, they were subsequently labeled with the following antibodies: 1:400 CD31-PE (clone 390; eBiosciences, San Diego, CA), 1:400 CD45-PE (clone 30-F11; BD Biosciences, San Jose, CA), and 1:4000 Sca-1-PE-Cy7 (clone D7; BD Biosciences, Vancouver, Canada). Fluorescence-activated cell sorting (FACS) was performed using a BD FACSAria II cell sorter (Becton-Dickinson, http://www.bd.com, Franklin Lakes, NJ) at the Emory University School of Medicine Core Facility for Flow Cytometry. Analyses of flow cytometry data were performed using FACSDiva (BD version 8.0.1).

FAP culture

FACS-purified FAPs were plated at 30,000 to 60,000 cells per well in a 6-well plate coated with collagen and cultured in DMEM supplemented with 20% FBS, 1% penicillin, and 2.5 ng/ml

bFGF (BioLegend, #579604) inside an incubator with 5% CO_2 (HERAcell VIOS 160i CO_2 incubator, Thermo Fisher Scientific, Waltham, MA) until the cells reached 70% confluency. Media was changed every 2-3 days.

Gene expression analysis by qPCR

FAPs of tongue muscles were analyzed for the expression of related markers using comparative qPCR. RNA from samples was extracted using Trizol (Invitrogen) according to the manufacturer's instructions. Isolated RNA (250 ng) was reverse transcripted into complementary DNA (cDNA) using random hexamers and M-MLV reverse transcriptase (Invitrogen) and then analyzed by real-time qPCR. The cDNA was amplified using Power SYBR® Green Master Mix (Applied Biosystems, Waltham, MA) and 2.5 μM of each primer. All primer sequences are listed in Supplemental Table 1. PCR reactions were performed for 35 cycles under the following conditions: denaturation at 95°C for 15 sec and annealing at 60°C for 1 min. Quantitative levels for all genes were normalized to endogenous *Gapdh* expression. Fold change of gene expression was determined using the ΔΔCt method (Livak & Schmittgen, 2001).

Immunohistochemistry/Immunofluorescence

Muscle sections were permeabilized with 0.5% Triton-X and blocked with 1% bovine serum albumin (BSA) and 5% donkey serum (blocking buffer) for 1 hour and labeled with primary antibodies overnight at 4 degree Celsius in 10% diluted blocking buffer in 0.2% Tween-20 in PBS (washing buffer). The following day, sections were washed three times with washing buffer and incubated with fluorescence probe-conjugated secondary antibodies for 1 hour at room temperature. Antibodies used are listed in Supplemental Table 2. Lipid droplets were stained with

HCS LipidTOX™ Green neutral lipid stain (Invitrogen) for 30 minutes with 1:200 dilution in PBS. Acetylcholine receptors were conjugated with 1 µg/mL α-bungarotoxin (αBTX) (Invitrogen) fluorescent for 30 minutes. Nuclei were stained with 1 µg/ml 4′,6-diamidino-2-phenylindole (DAPI). Before imaging, the staining was mounted with Vectashield (Vector Labs, www.vectorlabs.com, Burlingame, CA).

Adipocyte quantification analysis

Fat infiltration was quantified by counting adipocytes and measuring adipocyte area. Adipocytes present in the vertical and transverse muscles of the tongue were analyzed, and three or four representative sections were used. The tongue of 8-month-old ND- or HFD-fed male and female mice was analyzed. Quantification of adipocyte area was performed using FIJI.

Neuromuscular junction (NMJ) denervation analysis

Z-stack images of 30 µm thick longitudinal tongue sections were captured using the Nikon AX/AX R Confocal Microscope System (Nikon), and reconstructed images were displayed by maximum intensity projection using the Nikon NIS-Elements platform (Nikon). For denervation assessment, we analyzed 100-150 NMJs located in the genioglossus muscle per tongue muscle. The numbers of completely denervated, partially denervated, and innervated NMJs were counted.

Statistical Analyses

Statistical analysis was performed using Prism 9.0. Statistical testing was performed using the unpaired two-tailed Student's t-test or ANOVA, as stated in the figure legends. P-value <0.05 is considered statistical significance. Error bars represent the mean ± SEM.

RESULTS

Hypertrophy of Adipocytes Causes Fatty Tongue in HFD-Induced Obese Mice

We aimed to investigate the role of HFD in promoting fat accumulation in the tongue, a phenomenon that has been observed in patients with OSA (A. M. Kim et al., 2014). We placed wild-type (WT) mice on a six-month diet-induced obesity course and observed marked weight gain (Fig. 1A). We then examined the adiposity of the tongue base in both ND and HFD groups and found unilocular adipocytes, particularly in the vertical and transverse muscles of the tongue (Fig. 1B). We confirmed their identity by immunostaining of perilipin-1, a mature adipocyte marker (Greenberg et al., 1991), and lipidTOX, a neutral lipid droplet marker (Miggitsch et al., 2019) (Fig. 1C). We found that in both males and females, there was an increase in the percentage of tongue cross-sectional area (CSA) occupied by adipocytes (Fig. 1D and 1G). To determine whether the increased fat area was caused by the increased size of adipocytes (hypertrophy) or by the increased number of adipocytes (hyperplasia), we measured the size and number of adipocytes in tongue sections. The average single adipocyte CSA was two times larger in HFD groups indicating hypertrophy of adipocytes by HFD (Fig. 1E and 1H); however, there was no significant difference in adipocyte number between ND and HFD groups in both males and females, indicating no hyperplasia by HFD (Fig 1F and 1I). This is also confirmed by adipocyte size distribution profiling comparing ND and HFD tongue muscles. Adipocyte size distribution of the HFD tongue shifted to the right, larger size, in both males and females compared to ND, indicating hypertrophy of adipocytes by HFD (Fig. 1E and 1H).

Since OSA is more prevalent in males than females, we analyzed if adipocyte hypertrophy shows sex differences. We performed a 2-way ANOVA analysis, which revealed that diet, but not sex, was the main factor affecting adipocyte hypertrophy and fatty tongue in obese mice. 2-way

ANOVA analysis of % adipocyte area revealed a significant difference between ND and HFD groups (column factor p=0.0121) but no significant difference between males and females (row factor p=0.2622) (Fig. S1A); also, average single adipocyte CSA revealed a significant difference between ND and HFD groups (column factor p=0.0020), but no significant difference between males and females (row factor p=0.5960) (Fig. S1B). 2-way ANOVA analysis of adipocyte number showed no significant difference between males and females (p=0.2047) and between ND and HFD groups (p=0.4708; Fig. S1C). Together, these results indicate that the primary factor contributing to the development of fatty tongue in obese mice is HFD-induced hypertrophy of adipocytes without sex differences in mouse.

HFD-induced Obesity Compromises Tongue Muscle NMJ Integrity

While an enlarged tongue is a known contributing factor (A. M. Kim et al., 2014), reduced tongue muscle tone during sleep can also lead to tongue collapse and OSA. To investigate the impact of HFD on the NMJ integrity of the tongue, we examined the integration of NMJs in the genioglossus muscle (Fig. 2A), a main muscle responsible for tongue protrusion and positioning. Using immunostaining for presynaptic (neurofilament) and postsynaptic regions (acetylcholine receptor) (Fig. 2B), we observed compromised NMJ integrity in the tongue muscle of mice fed HFD for six months (Fig. 2C). This effect was significant in males, with a higher percentage of denervated NMJs compared to those fed an ND (Fig. 2C and 2D). Our findings suggest that HFD-induced obesity impairs neuromuscular connection in the tongue muscle, contributing to tongue collapse and potentially OSA.

HFD-induced Obesity Affects Tongue Function in Female Mice

To monitor the functional consequences of increased fat and denervation of NMJs on tongue movement, we measured lick speed (tongue protrusions/second) in WT mice that were placed on a 6-month HFD feeding. Results showed that only female mice exhibited a slightly decreased lick speed, while males did not show significant changes (Fig. 3A). We used a genetic mouse model for obesity and type II diabetes known as the *db/db* mouse for this study. Obesity and type II diabetes are highly correlated to OSA (Foster et al., 2009), (Muraki, Wada, & Tanigawa, 2018). Although we did not examine the NMJ of the *db/db* mice, they exhibited a decrease in lick speed, showing potential as an OSA model (Fig. 3B). This suggests that HFD-induced obesity slightly impedes tongue motion, which could have implications for the development of OSA in humans.

Bmp3b Expression in FAPs as a Possible Factor to Induce Adipocyte Hypertrophy and NMJ Degeneration in Obese Mice

The mechanism underlying the simultaneous enlargement of adipocytes and denervation of NMJs in the tongue of obese mice remains unclear. To explore this, we focused on BMP3b, which is highly expressed in FAPs, and its deficiency has been linked to muscle mass loss and NMJ degeneration (Uezumi et al., 2021). Studies have also shown that overexpression of *Bmp3b* can protect against HFD-induced adipocyte hypertrophy, while a deficiency of *Bmp3b* is associated with adipocyte hypertrophy (Martí-Pàmies et al., 2020). Therefore, we hypothesized that decreased expression of *Bmp3b* in FAPs could be responsible for both adipocyte hypertrophy and NMJ degeneration in the tongue of obese mice. To test this hypothesis, we analyzed the expression of *Bmp3b* in FAPs isolated from the tongue muscles of ND and HFD-fed mice. Our results revealed that *Bmp3b* expression was significantly lower in obese female mice fed on an HFD, and this was

observed in both the tongue and gastrocnemius (GA) muscles (Fig. 4A). Additionally, *Bmp3b* expression was lower in male mice compared to female mice (Fig. 4B). This observation suggests that the reason for males being more susceptible to OSA could be due to this decreased in *Bmp3b* expression. These findings suggest that *Bmp3b* genes could be regulated by HFD, and further studies will focus on exploring the epigenetic regulation of *Bmp3b*, such as promoter methylation, microRNA regulation, or m6A RNA modification. These results provide valuable insights into the molecular mechanisms underlying obesity-induced fatty tongue and loss of NMJ integrity in the tongues of obese subjects.

DISCUSSION

In recent years, the prevalence of OSA has been increasing (Franklin & Lindberg, 2015; Peppard et al., 2013), but the cellular and molecular mechanisms causing OSA have yet to be researched. Obesity-induced fat deposition in the tongue of OSA patients has been proposed as a link between obesity and OSA (A. M. Kim et al., 2014; Wang et al., 2020), and our study provides the cellular role of FAPs in response to obesity in tongue muscle. Our results showed HFD-induced denervation at NMJs and hypertrophy of adipocytes in the tongue muscles of mice. We also found that FAP-derived BMP-3b may be the driving factor behind these changes. This sheds light on the complex interplay between muscle remodeling, fat deposition, and denervation in the tongue in response to obesity. Our study also provides new insights into the role of FAPs in maintaining NMJs and potentially contributing to OSA in obese patients. By understanding the multifaceted roles of FAPs in tongue muscle tissue, we may be able to identify new therapeutic targets for treating OSA and other pathophysiological conditions related to muscle dysfunction.

Our study presents an innovative approach to investigating the pathophysiology of OSA by creating an animal model of obesity-induced fatty tongue in mice, which offers several advantages. First, our model provides a tool to study the cause of fatty and denervated tongue muscles as a tissue model of OSA, which cannot be explored by mimicking OSA by intermittent hypoxia (Trzepizur et al., 2018) in animals that only provide consequences of OSA. Second, the diet-induced obese model is physiologically relevant and more valuable compared to genetic models of obesity, such as the *db/db* or *ob/ob* model, as it more closely mimics the human behavior of becoming obese in the absence of genetic modification. However, our study is limited by the fact that we only examined the tongue muscle, while other muscles, such as the pharyngeal muscles or soft palate, also contribute to OSA. Overall, our findings provide important insights into the

mechanisms underlying fatty tongue development in obesity and offer a new perspective for developing therapeutic interventions for OSA.

OSA is known to be more common in men than women, with male dominance of up to three-fold (Quintana-Gallego et al., 2004). Moreover, research indicates that male mice are more vulnerable to the long-term effects of an HFD on NMJ damage than female mice (Martinez-Pena & Akaaboune, 2020). Interestingly, our data aligns with these findings, as we have discovered that male mice had lower levels of *Bmp3b* expression in FAPs from tongue muscles compared to female mice, which suggests that there may be sex differences in the molecular mechanisms underlying the denervation of NMJs in response to obesity, further male prevalence of OSA. However, sex differences in adipocyte hypertrophy in tongue muscles were not observed. Further investigating these differences may provide valuable insights into potential sex-specific therapeutic targets for OSA treatment.

In conclusion, our study established the HFD-induced high-fat tongue as a valuable preclinical tissue model to investigate OSA. Our findings provided new insights into the adipogenic and neuromuscular remodeling of the tongue muscle in response to HFD-induced obesity, indicating the involvement of FAPs-derived BMP-3b in developing OSA. Our study's findings could be further explored in future research, including investigating the underlying mechanisms of HFD regulation of BMP-3b expression and testing potential therapeutic targets that target BMP-3b in treating OSA and other conditions related to muscle dysfunction. Overall, our research contributes to a better understanding of the complex interplay between muscle remodeling, fat deposition, and denervation in the tongue in response to obesity, providing a foundation for developing more effective treatment strategies for OSA.

Author contributions

AK was involved in designing the study, conducting experiments, analyzing data, performing image analysis, creating figures, and writing the thesis. FW conducted experiments. HJC provided overall guidance and was involved in study design and thesis revision.

Conflict of interest

The authors state that there are no conflicts of interest.

Data availability

All data to support the conclusions of this manuscript are included in the main text and supplementary materials.

REFERENCES

Benjafield, A. V., Ayas, N. T., Eastwood, P. R., Heinzer, R., Ip, M. S. M., Morrell, M. J., . . . Malhotra, A. (2019). Estimation of the global prevalence and burden of obstructive sleep apnoea: a literature-based analysis. (2213-2619 (Electronic)).

Cheung, T. H., Quach, N. L., Charville, G. W., Liu, L., Park, L., Edalati, A., . . . Rando, T. A. (2012). Maintenance of muscle stem-cell quiescence by microRNA-489. *Nature, 482*(7386), 524-528. doi:10.1038/nature10834

Foster, G. D., Borradaile, K. E., Sanders, M. H., Millman, R., Zammit, G., Newman, A. B., . . . Kuna, S. T. (2009). A randomized study on the effect of weight loss on obstructive sleep apnea among obese patients with type 2 diabetes: the Sleep AHEAD study. *Arch Intern Med, 169*(17), 1619-1626. doi:10.1001/archinternmed.2009.266

Franklin, K. A., & Lindberg, E. (2015). Obstructive sleep apnea is a common disorder in the population-a review on the epidemiology of sleep apnea. *J Thorac Dis, 7*(8), 1311-1322. doi:10.3978/j.issn.2072-1439.2015.06.11

Greenberg, A. S., Egan, J. J., Wek, S. A., Garty, N. B., Blanchette-Mackie, E. J., & Londos, C. (1991). Perilipin, a major hormonally regulated adipocyte-specific phosphoprotein associated with the periphery of lipid storage droplets. *J Biol Chem, 266*(17), 11341-11346.

Hino, J., Kangawa, K., Matsuo, H., Nohno, T., & Nishimatsu, S. (2004). Bone morphogenetic protein-3 family members and their biological functions. *Front Biosci, 9*, 1520-1529. doi:10.2741/1355

Javaheri, S., Barbe, F., Campos-Rodriguez, F., Dempsey, J. A., Khayat, R., Javaheri, S., . . . Somers, V. K. (2017). Sleep Apnea: Types, Mechanisms, and Clinical Cardiovascular Consequences. (1558-3597 (Electronic)).

Kim, A. M., Keenan, B. T., Jackson, N., Chan, E. L., Staley, B., Poptani, H., . . . Schwab, R. J. Tongue fat and its relationship to obstructive sleep apnea. (1550-9109 (Electronic)).

Kim, A. M., Keenan, B. T., Jackson, N., Chan, E. L., Staley, B., Poptani, H., . . . Schwab, R. J. (2014). Tongue fat and its relationship to obstructive sleep apnea. *Sleep, 37*(10), 1639-1648. doi:10.5665/sleep.4072

Kim, E., Wu, F., Lim, D., Zeuthen, C., Zhang, Y., Allen, J., . . . Choo, H. J. (2022). Fibroadipogenic Progenitors Regulate the Basal Proliferation of Satellite Cells and Homeostasis of Pharyngeal Muscles via HGF Secretion. *Front Cell Dev Biol, 10*, 875209. doi:10.3389/fcell.2022.875209

Kurosawa, T., Minato, K., Ikemoto-Uezumi, M., Hino, J., Tsuchida, K., & Uezumi, A. (2021). Transgenic Expression of Bmp3b in Mesenchymal Progenitors Mitigates Age-Related Muscle Mass Loss and Neuromuscular Junction Degeneration. *Int J Mol Sci, 22*(19). doi:10.3390/ijms221910246

Livak, K. J., & Schmittgen, T. D. (2001). Analysis of relative gene expression data using real-time quantitative PCR and the 2(-Delta Delta C(T)) Method. *Methods, 25*(4), 402-408. doi:10.1006/meth.2001.1262

Marshall, N. S., Wong Kk Fau - Liu, P. Y., Liu Py Fau - Cullen, S. R. J., Cullen Sr Fau - Knuiman, M. W., Knuiman Mw Fau - Grunstein, R. R., & Grunstein, R. R. (2019). Sleep apnea as an independent risk factor for all-cause mortality: the Busselton Health Study. (0161-8105 (Print)).

Martí-Pàmies, Í., Thoonen, R., Seale, P., Vite, A., Caplan, A., Tamez, J., . . . Scherrer-Crosbie, M. (2020). Deficiency of bone morphogenetic protein-3b induces metabolic syndrome and increases adipogenesis. *Am J Physiol Endocrinol Metab, 319*(2), E363-e375. doi:10.1152/ajpendo.00362.2019

Martinez-Pena, Y. V. I., & Akaaboune, M. (2020). The disassembly of the neuromuscular synapse in high-fat diet-induced obese male mice. *Mol Metab, 36*, 100979. doi:10.1016/j.molmet.2020.100979

Miggitsch, C., Meryk, A., Naismith, E., Pangrazzi, L., Ejaz, A., Jenewein, B., . . . Grubeck-Loebenstein, B. (2019). Human bone marrow adipocytes display distinct immune regulatory properties. *EBioMedicine, 46*, 387-398. doi:10.1016/j.ebiom.2019.07.023

Muraki, I., Wada, H., & Tanigawa, T. (2018). Sleep apnea and type 2 diabetes. *J Diabetes Investig, 9*(5), 991-997. doi:10.1111/jdi.12823

Peppard, P. E., Young, T., Barnet, J. H., Palta, M., Hagen, E. W., & Hla, K. M. (2013). Increased prevalence of sleep-disordered breathing in adults. *Am J Epidemiol, 177*(9), 1006-1014. doi:10.1093/aje/kws342

Quintana-Gallego, E., Carmona-Bernal, C., Capote, F., Sánchez-Armengol, A., Botebol-Benhamou, G., Polo-Padillo, J., & Castillo-Gómez, J. (2004). Gender differences in obstructive sleep apnea syndrome: a clinical study of 1166 patients. *Respir Med, 98*(10), 984-989. doi:10.1016/j.rmed.2004.03.002

Trzepizur, W., Cortese, R., & Gozal, D. (2018). Murine models of sleep apnea: functional implications of altered macrophage polarity and epigenetic modifications in adipose and vascular tissues. *Metabolism, 84*, 44-55. doi:10.1016/j.metabol.2017.11.008

Uezumi, A., Ikemoto-Uezumi, M., Zhou, H., Kurosawa, T., Yoshimoto, Y., Nakatani, M., . . . Tsuchida, K. (2021). Mesenchymal Bmp3b expression maintains skeletal muscle integrity and decreases in age-related sarcopenia. *J Clin Invest, 131*(1). doi:10.1172/jci139617

Wang, S. H., Keenan, B. T., Wiemken, A., Zang, Y., Staley, B., Sarwer, D. B., . . . Schwab, R. J. (2020). Effect of Weight Loss on Upper Airway Anatomy and the Apnea-Hypopnea Index. The Importance of Tongue Fat. *Am J Respir Crit Care Med, 201*(6), 718-727. doi:10.1164/rccm.201903-0692OC

FIGURE LEGENDS

Figure 1. Hypertrophy of Adipocytes Causes Fatty Tongue in HFD-Induced Obese Mice

(A) To generate a diet-induced obese mouse model, the control group received a normal diet (ND), which contains 13.5% calories from fat until eight weeks of age. Then, the control group continued ND while the experimental group switched to a high-fat diet (HFD) containing 42% calories from fat. Mice consumed the ND or HFD for six months before analyses, and body weight was measured every month. Both groups had wild type (C57BL/6). n=6-7 in ND male, n=9-14 in HFD male, n=5-15 in ND female, n=13-17 in HFD female. Statistical significance was determined by 2-way ANOVA. **(B)** Hematoxylin and Eosin (H&E) staining of tongue cross-sections of ND and HFD fed mouse. The left panel shows the entire tongue section, and the right panel shows the magnified image of the boxed region. Arrowheads indicate adipocytes. Scale bar = 400μm. **(C)** Immunostaining of tongue cross-sections of ND and HFD-fed mice for perilipin-1 (red), lipidTOX (green), and DAPI. Scale bar=170 μm. **(D-I)** Quantification of C. Red perilipin-stained adipocyte number was counted, and the area was measured. Red perilipin-stained adipocytes were counted, and their area was measured. The % adipocyte area was determined by adding up the total area occupied by adipocytes and dividing it by the total area of the tongue. The average adipocyte area was calculated by adding up the total area occupied by adipocytes and dividing it by the total adipocyte number. Statistical significance was determined by the student t-test. **(D)** % adipocyte area in males. **(E)** Average adipocyte area and its distribution in males. **(F)** Number of adipocytes in males. **(G)** % adipocyte area in females. **(H)** Average adipocyte area and its distribution in females. **(I)** Number of adipocytes in females. The p-values are shown above the horizontal line, which is positioned above the bars. Error bars represent the mean ± SEM.

Figure 2. HFD-induced Obesity Compromises Tongue Muscle NMJ Integrity

(A) Illustration of the genioglossus muscle (dark red). **(B)** Immunofluorescence staining of WT tongue longitudinal sections for neurofilament (NF) and acetylcholine receptor (αBTX). Arrowheads: NMJs. Red arrowhead: completely denervated NMJ. Green arrowhead: partially denervated NMJ. Yellow arrowhead: Innervated NMJ. Scale bar = 50μm. **(C)** Ratios of completely denervated, partially denervated), and innervated NMJ were calculated. All NMJs from 3 replicates were combined. **(D)** % of Completely denervated NMJs in ND and HFD-fed males. The p-values are shown above the horizontal line, which is positioned above the bars. Error bars represent the mean ± SEM. Statistical significance was determined by the student t-test.

Figure 3. HFD-induced Obesity Affects Tongue Function in Female Mice

The mice were given a water bottle with a sipper and two days to adjust to it. In order to increase their water consumption during the experiment, the mice were not given any water for 16 hours before the test. After that, the water bottles were reintroduced, and the lick events were recorded on video about 30 seconds later. **(A)** Lick rate of ND and HFD fed male and female mice. n=6-7 in the male ND group. n=7-8 in the male HFD group. n=8-9 in the female ND group. n=9-10 in the female HFD group. Statistical significance was determined by 2-way ANOVA. **(B)** Lick rate of the db/db mice. 4 male mice were used in each group. The p-values are shown above the horizontal line, which is positioned above the bars. Error bars represent the mean ± SEM. Statistical significance was determined by the student t-test.

Figure 4. Bmp3b Expression in FAPs as a Possible Factor to Induce Adipocyte Hypertrophy and NMJ Degeneration in Obese Mice

(A) *Bmp3b* expression is significantly decreased in HFD-fed obese mice in both tongue and GA. n=2-4 independent cultures. **(B)** *Bmp3b* expression is lower in males compared to females, in both tongue and GA. FAPs from ND-fed mice were used. n=2-4 independent cultures. The p-values are shown above the horizontal line, which is positioned above the bars. Error bars represent the mean ± SEM. Statistical significance was determined by the student t-test.

SUPPLEMENTAL FIGURE LEGENDS

Figure S1. High-Fat Diet-Induced Hypertrophy of Adipocytes Contributes to Fatty Tongue Development in Obese Mice Without Sex Differences

2-way ANOVA analysis of Figure 1 D-I. The row factor is sex, and the column factor is diet. **(A)** 2-way ANOVA analysis of % adipocyte area in males and females. **(B)** 2-way ANOVA analysis of the number of adipocytes in males and females. **(C)** 2-way ANOVA analysis of the number of adipocytes in males and females. The p-values are shown above the horizontal line, which is positioned above the bars. Error bars represent the mean ± SEM.

FIGURES

Figure 1. Hypertrophy of Adipocytes Causes Fatty Tongue in HFD-Induced Obese Mice

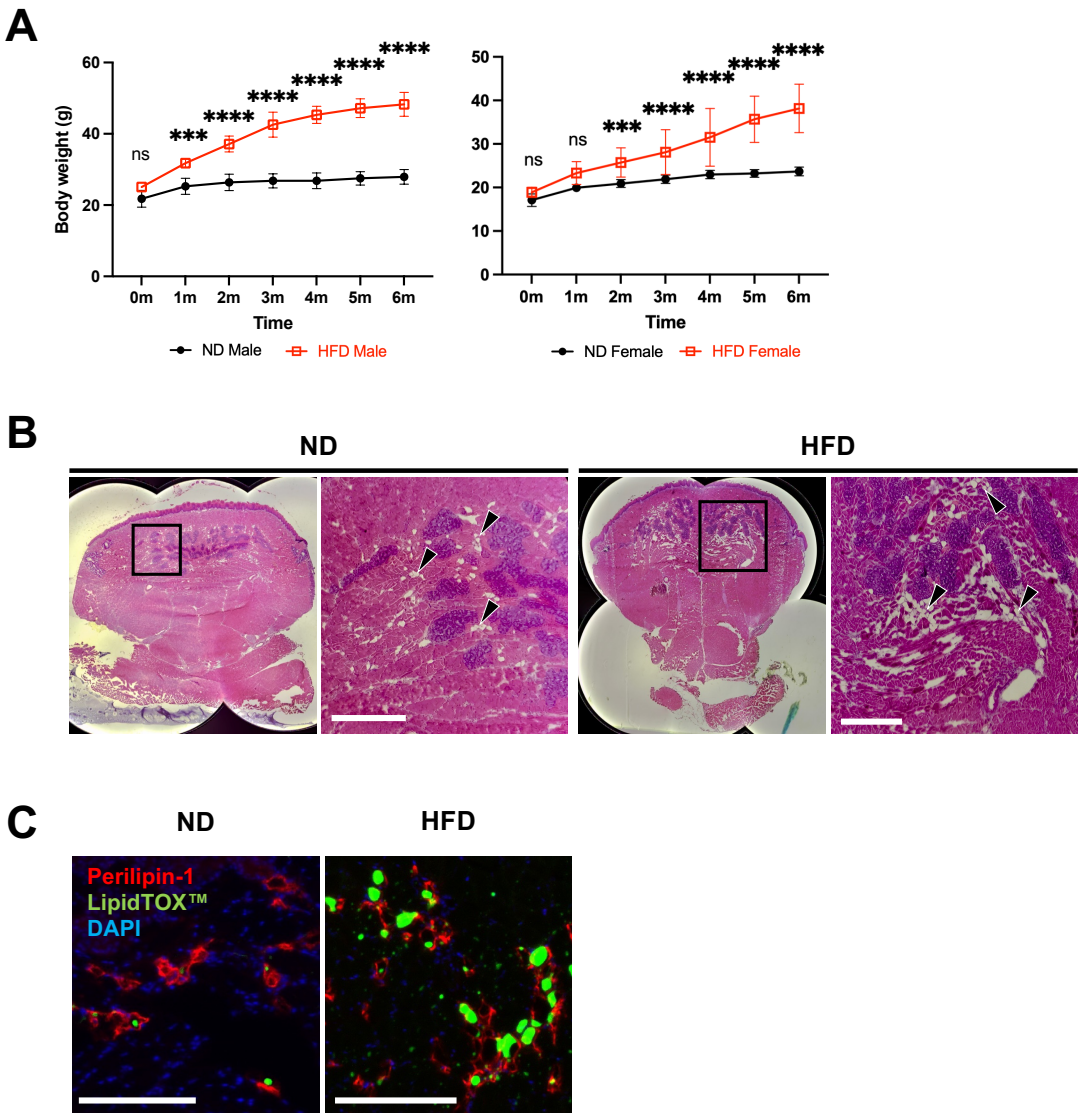

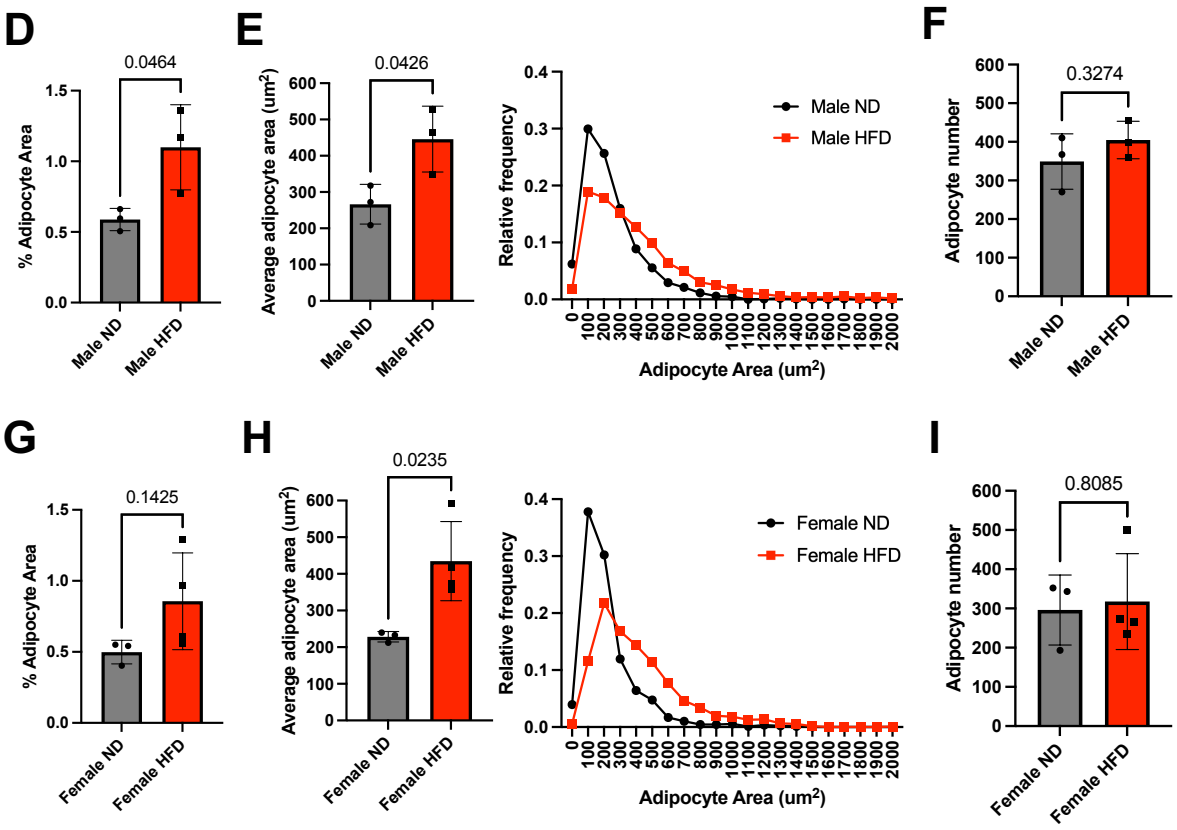
D
0.0464
% Adipocyte Area
Male ND
Male HFD
E
0.0426
Average adipocyte area (um2)
Male ND
Male HFD
Relative frequency
Male ND
Male HFD
Adipocyte Area (um2)
F
0.3274
Adipocyte number
Male ND
Male HFD
G
0.1425
% Adipocyte Area
Female ND
Female HFD
H
0.0235
Average adipocyte area (um2)
Female ND
Female HFD
Relative frequency
Female ND
Female HFD
Adipocyte Area (um2)
I
0.8085
Adipocyte number
Female ND
Female HFD

Figure 2. HFD-induced Obesity Compromises Tongue Muscle NMJ Integrity

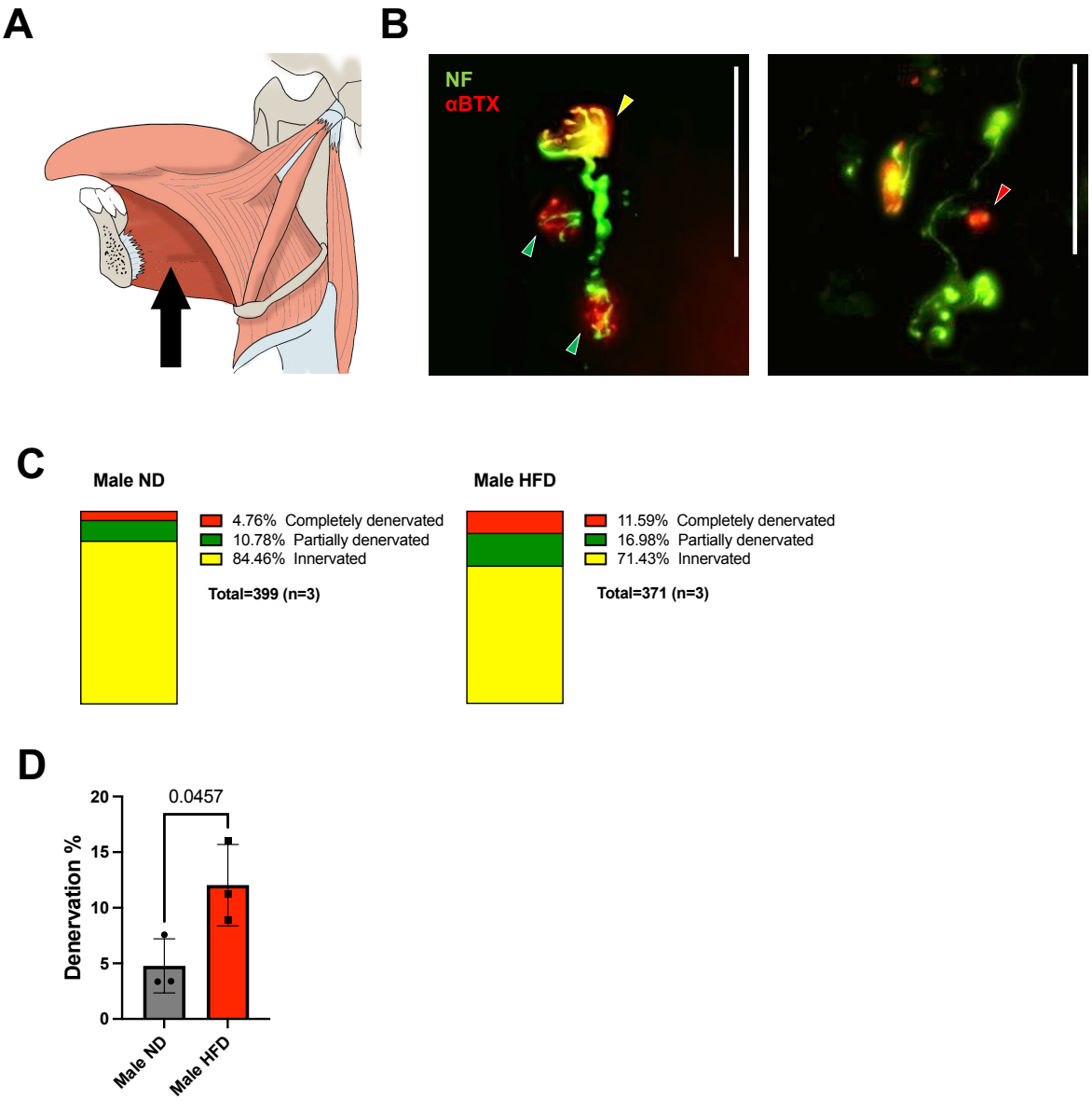

Figure 3. HFD-induced Obesity Affects Tongue Function in Female Mice

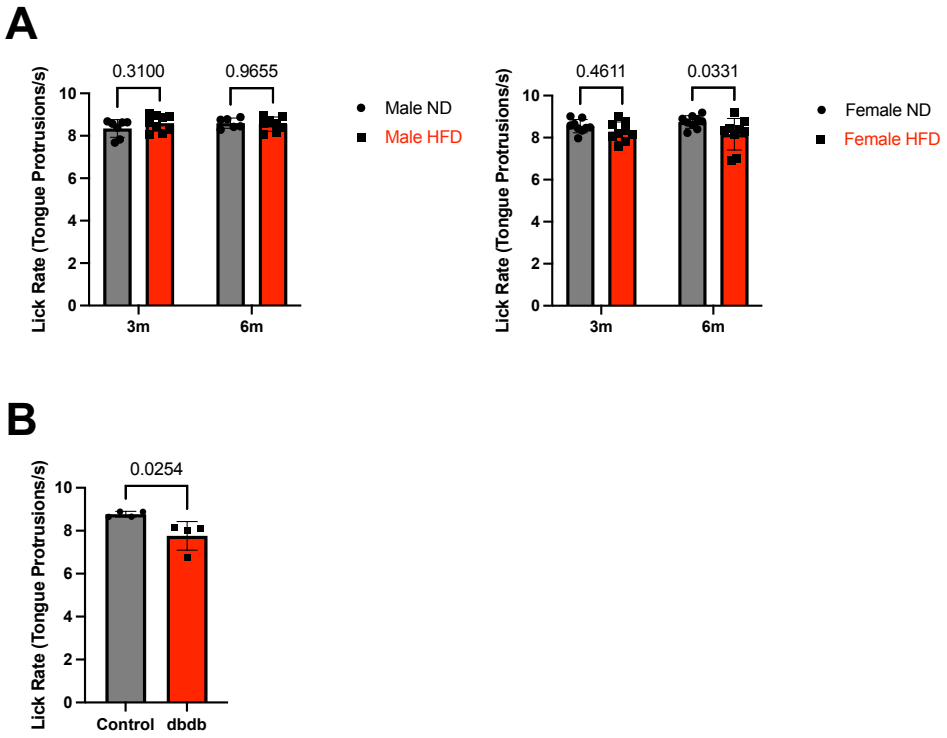

Figure 4. Bmp3b Expression in FAPs as a Possible Factor to Induce Adipocyte Hypertrophy and NMJ Degeneration in Obese Mice

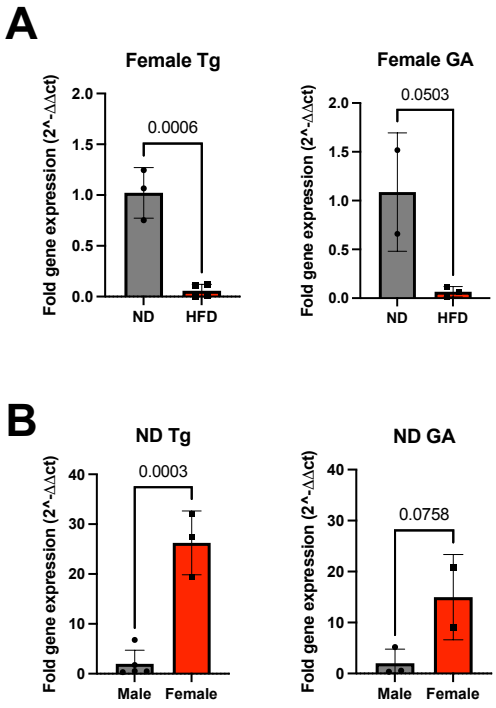

SUPPLEMENTAL MATERIAL

Supplemental Table 1 - Primer sequences used for qPCR

Genes	Primer Sequences
Bmp3b	5' - CTTTGACGCCTACTACTGTGCTG - 3'
	5' - AAGGGAGTTCATCTTGTCTGGAA -3'
Gapdh	5' - ACCACAGTCCATGCCATCAC - 3'
	5' - TCCACCACCCTGTTGCTGTA - 3'

Supplemental Table 2 - Antibodies used for immunohistochemistry

Primary antibody

Detection of	**Name**	**Host species**	**Dilution or Concentration**	**Manufacturer (Cat #)**
Adipocytes	Perilipin	Rabbit IgG	1:100	Sigma-Aldrich (P1873-200UL)
Neurofilament	SMI-32	Rabbit IgG	1:100	Abcam (ab72996)

Secondary Reagents

Secondary Reagent	**Conjugate(s)**	**Dilution**	**Manufacturer (Cat #)**
Donkey Anti-Rabbit IgG	Alexa Fluor® 594	1:200	Jackson ImmunoResearch (711-586-152)
Donkey Anti-Rabbit IgG	Fluorescein (FITC)	1:200	Jackson ImmunoResearch (711-096-152)

Figure S1. High-Fat Diet-Induced Hypertrophy of Adipocytes Contributes to Fatty Tongue Development in Obese Mice Without Sex Differences

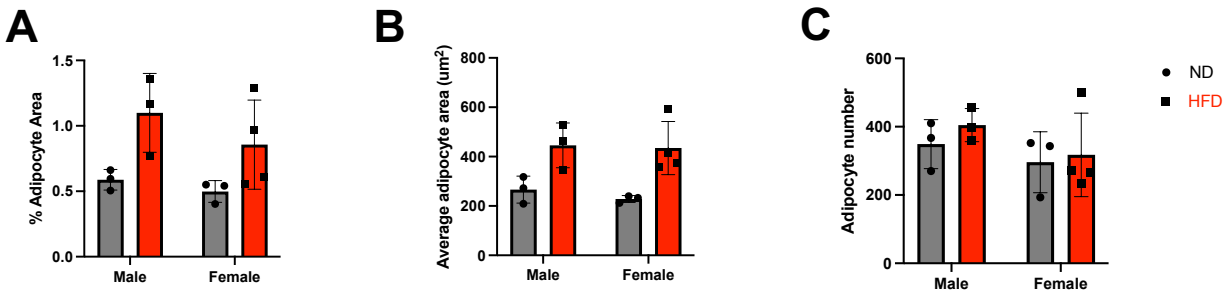

Source of Variation	% of total variation	P value
Interaction	1.540	0.5930
Row Factor (Sex)	7.174	0.2622
Column Factor (Diet)	49.08	0.0121

Source of Variation	% of total variation	P value
Interaction	0.3235	0.7704
Row Factor (Sex)	1.079	0.5960
Column Factor (Diet)	66.41	0.0020

Source of Variation	% of total variation	P value
Interaction	0.9700	0.7465
Row Factor (Sex)	16.33	0.2047
Column Factor (Diet)	4.948	0.4708